OPTIMA: A high time resolution optical photo-polarimeter

G. Kanbach[1], A. Stefanescu[1], S. Duscha[1], M. Mühlegger[1], F. Schrey[1], H. Steinle[1], A. Słowikowska[1,3], H. Spruit[2]

[1] Max Planck Institut für Extraterrestrische Physik, Postfach 1312, 85741 Garching, Germany gok@mpe.mpg.de, astefan@mpe.mpg.de, sduscha@mpe.mpg.de, mmuehleg@mpe.mpg.de, fzs@mpe.mpg.de, hcs@mpe.mpg.de

[2] Max Planck Institut für Astrophysik, Karl-Schwarzschild-Str. 1 85741 Garching, Germany henk@mpa-garching.mpg.de

[3] Nicolaus Copernicus Astronomical Center, Dept. of Astrophysics, Toruń, Poland aga@mpe.mpg.de or aga@ncac.torun.pl

1 Abstract

A high-speed photo-polarimeter, "OPTIMA" short for Optical Pulsar Timing Analyzer, has been designed and developed in the group for gamma-ray astronomy of the Max-Planck-Institut für extraterrestrische Physik. This sensitive, portable detector is used to observe optical emissions of sources that radiate mainly at X- and gamma-ray energies, like pulsars and other highly variable compact sources. The single photon counting instrument is based on fiber fed avalanche photodiodes (APDs), a GPS timing receiver, a CCD camera for target acquisition and a stand-alone data acquisition and control system. Several configurations are available: for photometry a hexagonal bundle with seven channels and one fiber offset for sky background monitoring; for polarimetry a rotating polarization filter in front of the photometer or a newly developed 4-channel double Wollaston system; and for coarse spectroscopy a 4-colour prism spectrograph.

2 General Layout

The concept of aperture timing photometry is very familiar to astronomers working in high-energy X- and gamma-ray astronomy. Single photon events are located on a sky map and their arrival times are registered. The desired target photons are then selected for analysis depending on their angular distance from the target source. In the optical band we can operate in the same way if a suitable fast 2 dimensional detector with single photon sensitivity is
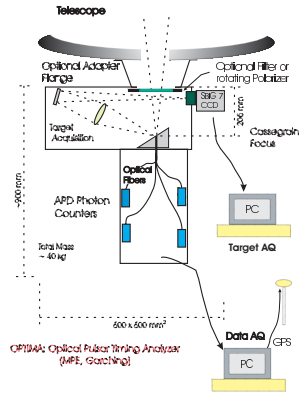
Fig. 1. Schematic layout of OPTIMA (pre-2006)

Fig. 2. Photograph of pre-2006 OPTIMA with open APD box of photon counters (3). The target acquisition optics (filters, target imaging and fiber pick-up) is located in box (1) and the CCD camera is mounted externally (2).
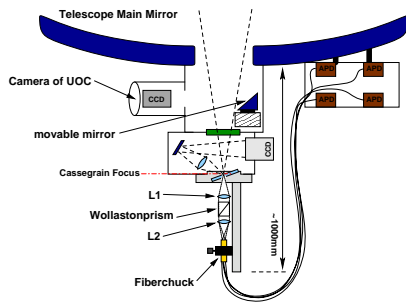
Fig. 3. Schematic layout of OPTIMA-Burst (since 2006)
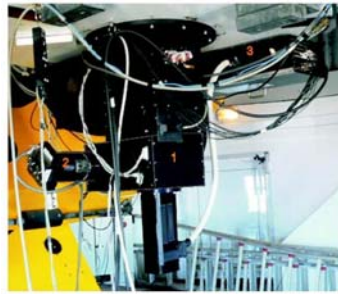
Fig. 4. Photograph of OPTIMA-Burst mounted to the Cassegrain focus of the Mt. Skinakas 1.3m telescope (UoC, Heraklion, Greece). The components are numbered like in figure 2.

available. Such detectors have been realized e.g. in the form of multi-anode micro-channel arrays (MAMA) on the TRIFFID camera [14] or as small, compact arrays of solid-state detectors (e.g. the Josephson junction detector S-Cam3 described by [9]). These cameras are still characterized by either low quantum efficiency or technically challenging operations. However they offer the advantages of imaging a larger field with fine resolution: event selection can be adapted to the seeing and sky background conditions and reference stars are often present in the same exposures.

Although the future will belong to advanced fast 2-D photon counting/timing cameras with high sensitivity (see e.g. the contribution by Strueder

et al., these proceedings), we have chosen to first develop a simple photon counting system ("OPTIMA" the Optical Pulsar Timing Analyzer) that relies on fixed apertures and is equipped with detectors of high quantum efficiency. The initial science goals were to measure optical pulsar lightcurves and highly variable binary systems and to establish timing relations to emissions in other wavelength ranges (radio and X-rays). For this purpose accurate quantitative photometry is not of prime importance and fixed apertures of an appropriate size are sufficient. The apertures are given by optical fibers which are placed in the focal plane of a telescope and feed the light of target stars and sky background to avalanche diode photon detectors (APDs). To ameliorate the negative aspects of fixed aperture photometry we installed an small 'integral field unit' of apertures in the form of a hexagonal close-packed bundle of fibers and a fast read-out for the field viewing acquisition CCD camera. The schematics of the OPTIMA detector (configuration up to 2005) and a photograph of the open system are shown in figures 1 and 2. Since 2006 a new OPTIMA configuration (called 'OPTIMA-Burst') is available. This configuration uses basically the components of the previous experiment but has a separate box for the APD detectors. The focal plane fibre pick-ups of the earlier version are also present in OPTIMA-Burst, but there is an additional aperture that inputs light into a new double-Wollaston polarimeter. All fibers (now of about 2m length) are fed through a semi-rigid tube to the APD box. Schematics and a photograph of OPTIMA-Burst are shown in figures 3 and 4.

We started to develop the OPTIMA photometer in 1998 ([20],[21]) and used progressively more complete systems on a 1.3m telescope (Mt. Skinakas, Crete), on the 3.5m telescope (Calar Alto, Spain), on the 2.1m Guillermo Haro telescope, Cananea, Mexico, the 2.5m NOT on La Palma, and, in the southern hemisphere, on the 74in Mt. Stromlo and 2.2m ESO/La Silla observatories. The new version OPTIMA-Burst has been used at the Skinakas observatory and early operations were described by [19] and [10].

2.1 Fiber pick-up and Detectors

OPTIMA intercepts the image formed in the focal plane of a large telescope with a slanted mirror. The reflected light is re-imaged on a commercial CCD camera. We currently use a fast-readout Apogee AP6 camera featuring a Kodak chip (type KAF1000E, 1024x1024 pixels of $24.4\mu m$ size, backside illuminated). A full frame is downloaded in about 1 sec. Embedded in the slanted mirror and coincident with the focal plane are the 'photon-counting' apertures (numbers 1-4 in figure 5) and 2 small LED lightsources (labelled A and B). These LEDs can be switched on via computer command and serve to control the overall alignment of the field-viewing optics and camera. Aperture no. 1 (size $\sim 345\mu m$) in fig.5 is the diaphragm for the double-Wollaston polarimeter. Opening no. 2, with 1.7mm diameter, contains the hexagonal fiber bundle mounted in a fine steel tube, and the apertures no. 3 and 4 respectively con-
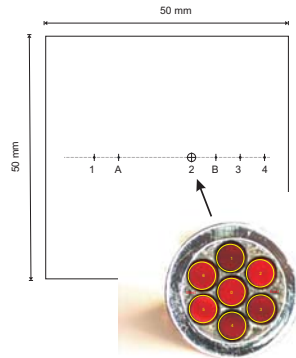
Fig. 5. Layout of the fiber input apertures in the field-viewing mirror (see text) and photograph of the hexagonal fiber bundle (input: single fiber diameter $\sim 320\mu m$; output diameter: $\sim 100\mu m$; length: 2m; illuminated from output side): central fiber for the target, ring fibers for the close-by sky or nebular environment.
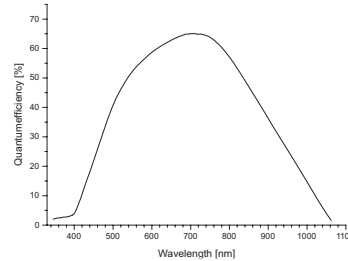
Fig. 6. Typical quantum efficiency of the Perkin-Elmer single photon counting modules SPCM-AQR-15-FC; dark noise ranging from 50 to 250 counts/sec.

tain a fiber input to a 4-channel prism spectrograph) and a fiber to record the night sky brightness near to the target. The field-viewing optics shows a region of approximately 12'x12' (at the telescope of Mt. Skinakas, Greece, f-ratio 7.64, D=129cm) with some vignetting near the edges. The main task of this system is to acquire the target star and to derive the telescope control commands to move the target into any chosen aperture. During the photon counting measurements, when the telescope guiding is controlled by an external auto-guider, the secondary task of the OPTIMA CCD is to take serial images of the field with short integration times (typically 10 sec). This series of exposures is evaluated for the atmospheric seeing and transparency conditions during the measurement.

For the photon-counting observation of faint sources it is very important to convert the highest possible fraction of incoming photons into countable signals. This efficiency should include the light losses on all optical surfaces (input to the fibres through a polished surface and coupling of the fiber into the optics included in the photon counting modules, each $\sim 4\%$), absorption in the fiber (very small for the chosen quartz fibers), and losses incurred by the taper that reduces fiber diameter from about $300\mu m$ (input) to $100\mu m$ (output). The 'optical' efficiency of the tapered fibers is not easily calibrated. Measurements by [20] estimated the fiber efficiency to be around 90% . Finally the quantum efficiency of the detectors should be large over a wide spectral band. Most previous systems for recording single optical photons with good

time resolution used photomultiplier tubes or detectors based on a similar technology with photo cathodes of peak quantum efficieny of typically 20% and a narrow wavelength range of sensitivity. Much better quantum efficiencies can be reached with solid state detectors. OPTIMA uses Avalanche Photodiodes (APDs). These silicon devices have been produced with peak quantum efficiencies of up to 80% and a wide band of sensitivity ranging from 250 to 1100 nm. We use commercially available APD based single photon counting modules of type SPCM-AQR-15-FC produced by Perkin-Elmer. These highly integrated devices operate in a Geiger counter mode where a photon initiated avalanche pulse is quenched by the instantaneous reduction of the bias voltage. The diodes have a diameter of 200μm and are electrically cooled with Peletier elements. The selected units offer low dark count rates of typically less than 50 cps, are insensitive to electromagnetic interference and are very reliable. They can record photons up to rates of $\sim 2 \times 10^6$ cps before noticeable deadtime losses occur. The present data acquisition however can not keep up with such rates. Typical DAQ event losses around 1% are encountered for rates of 4×10^4 cps. The achieved quantum efficiency of the APD detectors is shown in figure 6. Although it falls short of the values mentioned above, it is still above 20% for a spectral range from 450 to 950 nm. Bandwidth and quantum efficiency of APDs results in about a factor of 6 improvement in sensitivity compared to PMT based systems.

2.2 Timing, Data Acquisition, and Software

The signals provided by the global positioning system (GPS) supply a global absolute time base. We use a receiver (from Datum Inc.) which can process the clock pulses of up to six satellites simultaneously and reaches an absolute time accuracy of better than $2\mu s$ on the "pulse per second (PPS)" GPS signal. This signal disciplines a local high frequency oscillator (250 kHz, i.e. leading to a time resolution window of $4\mu s$) with the same precision which provides a continuous UTC time signal to the system bus of the PC used for data acquisition (DAQ). The task of the DAQ unit is thus to correlate the electronic signals of the APD detector modules with the high resolution time base and assign UTC arrival times to each detected photon. The timing of the conversion cycles of the DAQ card is controlled by the GPS based oscillator, so that the transfer of the APD detector signals is running at a fixed rate. The absolute starting time of each software triggered acquisition sequence is precisely known. The controlling software counts the number of conversion cycles since the start of the sequence and stores this sequential number together with an identifier of the respective detector channel for each detected photon. Conversion cycles without detected photons are skipped. Based on the cycle number, the acquisition frequency and the absolute time of the start of the sequence the UTC arrival time of every recorded photon can be restored during data analysis. During the long-term measurements the consistency and continuity of the time base are continously controlled. The presently used DAQ

system is limited to rates below about $\sim 10^5$ cps because of pile-up in the time-resolution window. Future versions of the DAQ should be able to control higher rates, which are achievable with the photon counters (up to several MHz).

Typical count rates from the night sky in dark conditions are $\sim 1 - 2$ kHz per fiber resulting in several GBytes of data for a night of observing. Data are first staged to RAM and periodically ($\sim$ every 10 mins.) stored on HDD. Off-line data analysis includes the options to transfer the topocentric photon arrival times to the solar system barycenter. Pulsar phases and light curves can be calculated if the pulsar ephemeris is known. If unknown periodicities or irregular variations are investigated FFT analysis and rate plots are available.

2.3 Polarimetry and Spectroscopy

Two versions of polarimetry were developed in order to extend the observational modes of the originally photometric instrument. The first polarimeter was realized with a rotating polaroid filter that modulates the complete field-of-view with all photon counting apertures. This mode of operation is especially well suited to the measurement of a polarized source embedded in an extended polarized nebula, like the Crab pulsar, where simultaneous target and background polarization data can be taken with the fiber bundle array. The disadvantages of a rotating polaroid are the rather low transmission ($\sim 32\%$ for unpolarized white light) and the fact that the polarization measurements are done in sequence as the the filter turns. The latter property restricts the use of this system to targets with slowly variable (with respect to the filter rotation rate of about 3 Hz) or regular periodic polarization. Irregular transient sources need to be measured with a system that offers parallel simultaneous polarimeters. This is the second variant of polarimeter, a double Wollaston system, that is available for OPTIMA.

Rotating Polaroid Filter

Figure 7 shows a photograph of the polarizer seen from top (telescope side) and bottom. The device can be introduced into the incoming beam above the fiber pick-up so that all fiber channels and the CCD image are fully covered. The polarizing filter (Type 10K by Spindler & Hoyer) is mounted on a precision roller bearing and is rotated with the motor visible on the bottom view. Typical rotation frequencies of up to 10 Hz can be adjusted through the supply voltage of the motor. Incoming linearly polarized light is modulated at twice the rotation frequency. In the top view a magnetic switch (magnet on the rotating filter, Hall sensor on the base plate) can be seen. The reference position of the filter is given by a signal from the Hall sensor. It is registered and timed in the same way as a photon event and stored in a separate channel. This allows interpolation of the position of the polarizing filter for any event using the time difference from the preceding and to the following Hall sensor

Fig. 7. Photograph of the OPTIMA rotating polarization filter. Left (seen from telescope side): 2: permanent magnet on rotating filter; the polarization direction of the filter (4) is perpendicular to the radius vector to the magnet. 3: Hall sensor on base plate. The filter rotates from north to east. Right: motor and belt. Typical rotation rates are 3-4 Hz.

signal. Slight irregularities in the rotation frequency of the RPF that occur on time-scales longer than fractions of a second, e.g. due to supply voltage drifts or mechanical resistance changes in the bearing and motor, can be corrected with sufficient accuracy. We have tested the RPF in the lab with unpolarized and linearly polarized light to ensure and prove that the OPTIMA fibers and detectors have no intrinsic, systematic response to polarized light. If the incoming light is polarized the filter produces a sinusoidal modulation as it rotates.

Double Wollaston Polarimeter

Figure 8 shows the basic layout of the new polarimeter optics. The target star is positioned in a diaphragm (aperture of $\sim 345 \mu m$ in the field viewing mirror) and the emerging beam is collimated. Two quartz Wollaston prisms are positioned side by side in the collimated beam (separated by a thin opaque plate) so that about half of the beam falls on each prism. The polarized and symmetrically diverging output beams (divergence about 1°)are re-focussed onto a fiber pick-up where four regular tapered fibers are mounted in a chuck. For further detail refer to the work of [10]. The system has been verified in the lab with polarized and unpolarized light and was used on the Skinakas observatory during November 2005 and during a long campaign from July to September, 2006. From the 2005 measurements a verification on polarimetry standard stars and on the phase dependent polarization of the Crab pulsar were obtained for the new polarimeter. The data from the 2006 observations are not yet analyzed.
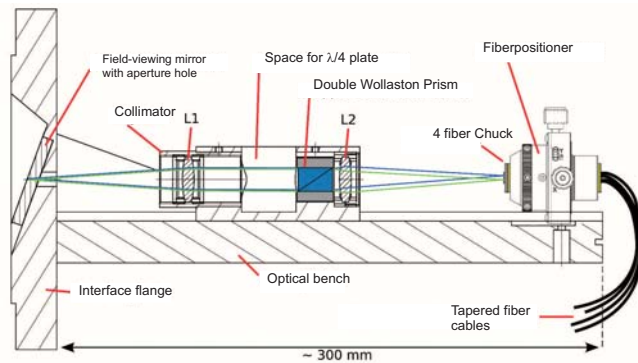
Fig. 8. Cut through the Double Wollaston Polarimeter. In the central parallel beam two Wollaston prisms, each covering about half the beam and separated by a thin opaque plate, split the incoming light into four images that are polarized at staggered angles $(0°, 45°, 90°,$ and $135°)$ and arranged approximately on the corners of a square.
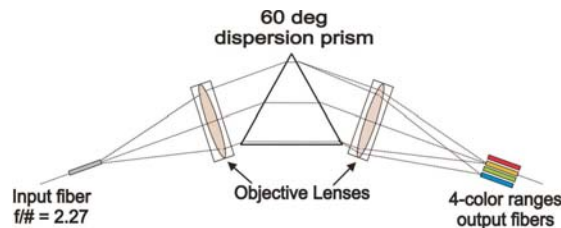
Fig. 9. Schematic of the prism spectrograph for simultaneous photometry in 4 colors

Prism Spectroscopy

A prism spectrograph with 4 output channels has been added as an option to the OPTIMA system. A schematic of the spectrometer is shown in Figure 9. The spectrometer fits in a small box and can be mounted inside the container with the photon counters. The input to the spectrometer is through a fiber from the telescope focal plane. The output spectrum spreads over about 1.1 mm for the wavelength range 500 to 900 nm. The output pick-up of 4 spectral bands consists of four 320μm fibers placed next to each other and mounted on a 3 axis micrometer stage. The position of the output fiber bundle in the spectrum then determines the spectral boundaries picked up by each "color" fiber. The overall efficiency of $\sim 5 - 10\%$ of this spectrometer is not very high, since the optics are of low quality and the fill factor of the pick-up fibers is small. It was primarily intended for use on rather bright source (e.g. Cyg X-1). The simultaneous fast timing of photons in several spectral bands could allow to investigate color variations during outbursts and timing correlations of photons with different energies.

3 Selected Measurements

The Crab Pulsar: single rotations and polarization

The Crab pulsar is the most widely used target in high-energy astronomy for instrument calibration and timing verification. OPTIMA was similarly used between 1999 and 2006 to verify the instrument and to perform scientific measurements of the optical emission from this young pulsar. Figure 10 shows an overlay of the OPTIMA bundle apertures on a HST image of the Crab pulsar (R. Romani, private communication and [11]). The scale in figure 10 corresponds to the plate scale of the NOT telescope (7.3 "/mm, 137 μm/"). About 0.65" southeast of the pulsar a knot of optical emission can be noted ([3]). Under ground-level seeing conditions this knot cannot be separated from the pulsar and it is clear that the measured intensity in the central fiber contains this light as well as the much brighter pulsar emissions. Figure 11 shows a trace of of the Crab light curve resolving single rotations with a time resolution of 1 ms. Folding the barycentric arrival times of the Crab with the rotational ephemerides derived from radio observations of Jodrell Bank [7] full agreement of the OPTIMA lightcurve with that derived from the high-speed photometer aboard the Hubble Space Telescope ([12]) was demonstrated ([21]). This confirms that OPTIMA introduces no detectable timing noise or other non-linear intensity responses to the optical signal of the pulsar. The stability of the OPTIMA timing system is demonstrated by the constancy of the Crab light curve as measured in many epochs.
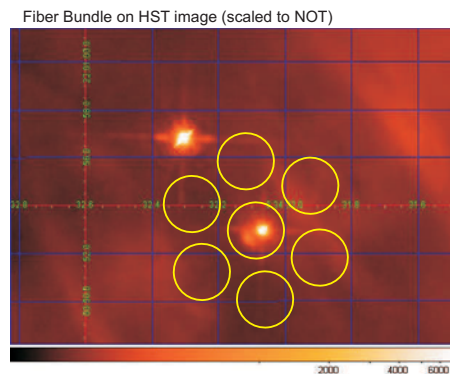
Fig. 10. Overlay of the OPTIMA fibre bundle on the Crab pulsar and its environment on a HST image. The scale (diameter of a fibre $\sim$ 2.3") corresponds to the focal plate scale of the 2.5m NOT telescope where observations were performed in Nov. 2003

For verification and in a first application of the rotating polaroid polarimeter we observed the Crab nebula and pulsar in January 2002 at Calar Alto
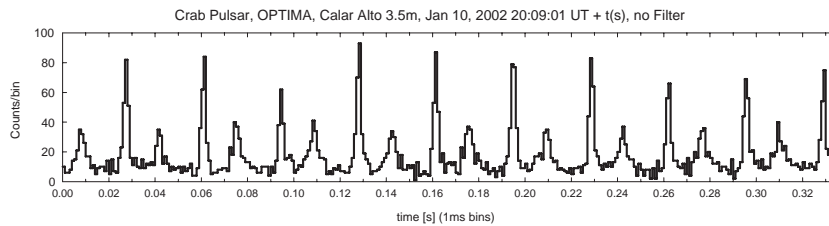
Fig. 11. Ten rotations of the Crab pulsar observed with 1ms time resolution at the 3.5m telescope on Calar Alto on 10 Jan 2002

using the 3.5m telescope. About 3 hours of exposure were achieved with the polarimeter ([6]). The analysis requires the separation of the highly polarized emission of the Crab nebula from the radiation of the pulsar point source. This is done with the fibers in the hexagonal bundle, where the central fiber is on the pulsar and the surrounding ring of fibers, at a distance of $\sim 2"$, record the nebular environment. All fibers include of course the sky background. Figure 10 plotted for the NOT focal plane scale (7.3 "/mm)which applies nearly also for the CAHA 3.5m telescope scale of 5.9"/mm. The nebular emission is then interpolated at the pulsar position from the ring of fibers. The Crab pulsar is detected at all phases of rotation, i.e. also in the so-called off-pulse phase with an intensity of about 1.2% (CAHA result [6], [5]) or about 2% (NOT result [15]) compared to the intensity of the first peak. This level could partly be explained by the presence of the unresolved inner knot, although a quantitative modelling has not yet been performed.

Preliminary polarization characteristics of the Crab pulsar were derived from the measurement ([6])and are shown in Figure 12. The degree of polarization and the position angle (PA) of the E-vector are plotted with a resolution of 500 phase bins. The result agrees generally well with the previous measurements [17], but shows details with much better definition and statistics. A measurement at the NOT in 2003 ([16] and [15]) accumulated about 25 hours of data. These results reveal much more details than all earlier measurements.

The interpretation of the optical polarization in terms of magnetospheric or pulsar wind emission models still involves an amount of uncertainty. The classical polar-cap and outer gap emission models fail to reproduce the observed polarization characteristics. Recent magnetospheric models like the two-pole caustic model ([1],[2]) predict qualitatively the large swings in the PA and the phases of the observed minima of polarization. Another approach places the optical emissions into the wind zone of the pulsar, where a magnetic field structure in the form of a tightly wound spiral streams from the pulsar ([13]). This model explains also some qualitative features of the data, especially the PA in the off-pulse phase: the wind streams out in the equatorial plane and the polarization should be oriented at an right angle, viz. aligned with the polar axis at an PA of about 120 degrees. The refined analysis and high statistics

data that are presently generated will certainly shed more light on the precise location and geometry of the optical radiation from the Crab pulsar.
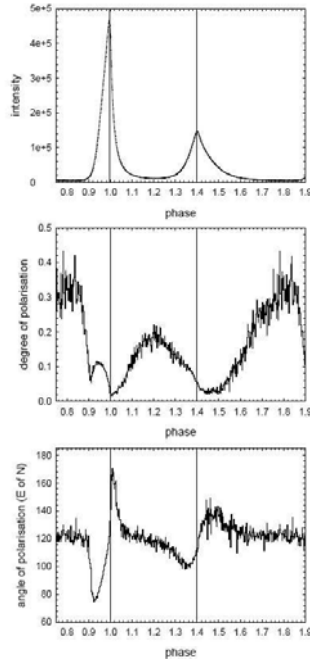
Fig. 12. Linear polarization of the Crab: the pulsar's rotation is divided in 500 intervals of about 70 μs duration ([6]).

Cataclysmic Variables: eclipsing AM Her binaries

The OPTIMA photometer was used to observe several short period binary systems. The selected targets were mostly of AM Her type and showed eclipses. As an example we present light curves for HU Aqr, which was observed repeatedly. HU Aqr is a close eclipsing binary system containing a highly magnetic white dwarf and a secondary star of type M4V. The orbital period is ~ 125 minutes. With a range of observed magnitudes from ~ 15 to 18 it is one of the brightest sources of this type. Very short timing signatures on the subsecond level were expected in this object, in particular at the eclipse entry and exit of the white dwarf. Figure 13 shows three sample lightcurves with 1 sec resolution measured on July 5, 2000, September 21, 2001, and July 18, 2004, respectively. Two eclipses of the white dwarf are the dominant features of these light curves. The sky background in the vicinity of the source has been subtracted using the hexagonal bundle of fibres. The low count rate level in

the eclipse is due to the secondary M4 star of magnitude 19.1^m. To describe some details of the light curve taken in July 2000 we start from the phase of mid-eclipse:
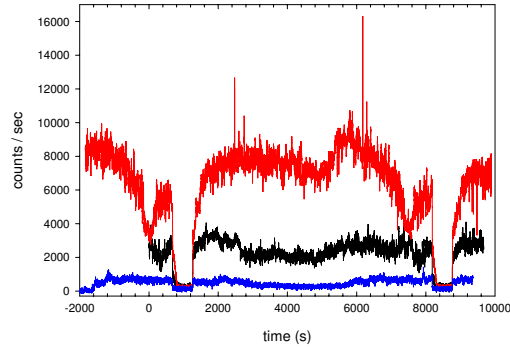
Fig. 13. Lightcurves with 1 sec resolution of the eclipsing cataclysmic variable HU Aqr at three epochs: Jul 5, 2000 (upper curve), Sep 21, 2001 (middle curve), and Jul 18, 2004 (lowest curve). The observations were taken at Skinakas observatory, Crete, Greece.

(1) the egress of the accretion spot has a duration of about 7 seconds. Using the orbital velocity of the white dwarf of ~ 200 km/s this duration corresponds to a spot size of about 1400 km. The same duration is observed at the ingress of the hot-spot into eclipse. (2) the high-intensity light curve shows two humps. This can be interpreted as the beaming pattern of cyclotron emission produced in the polar regions of the accretion column above the white dwarf. (3) sharp spikes of optical emission with clearly resolved time scales of 1-2 seconds and a brightness increase of up to a factor of 2. These features, observed for the first time, could be due to strong inhomogeneities in the mass accretion flow or to flaring outbursts from the surface. (4) before the eclipse a dip of the intensity is observed. This is explained as absorption as the accretion stream moves in front of the hot-spot on the white dwarf. The depth and orbital phase of this absorption dip indicate that in the July 2000 observation the mass accretion rate was unusually high while the later and shallower absorption in September 2001 points to a weak accretion stream. (5) after the precipitous entry of the hot-spot into eclipse, a gradually fading component can be detected. This is interpreted as the entry of the luminous parts of the accretion stream into eclipse behind the secondary star. The second observation in September 2001 showed an intensity of HU Aqr already at an level less than 25% of the 2000 values and the strong spikes in the light curve were not detected again. Later observations, like in 2004 and up to 2006, indicate that HU Aqr has faded even more and has not yet returned into a high intensity state.

The Black Hole binary transient KV UMa: correlation of X-ray and optical variability

From January to August 2000 the bright X-ray transient XTE J1118+48 (=KV UMa) was in an unusually long and intense state of outburst. This provided a unique opportunity for simultaneous X-ray and optical observations. KV UMa is a nearby binary system (∼2 kpc) at high galactic latitude and contains a compact star with more than 6 solar masses. OPTIMA was used on the 1.3m telescope at Skinakas observatory for a simultaneous exposure of 2.5 hours with RXTE over the nights of July 4-7, 2000 [4].

The variable emission from the black hole candidate was recorded with a timing accuracy of a few ms at X- and optical wavelengths. The X-ray to optical cross-correlation (Figure 14), shows that the optical emission rises suddenly following an increase in X-ray output. The positive optical response lags the X-rays by typically 500 ms with a very fast onset on a timescale of 30 ms. Although this delayed optical emission is suggestive of a reprocessing scenario (light echo), the autocorrelation of the X-ray and optical time series shows that the latter has intrinsically a much faster timing structure. This argues strongly against reprocessing. It is therefore proposed that the optical light is separately generated as cyclo-synchrotron emission in a region about 20000 km from the black hole. The delay is then explained as a time of flight delay of disturbances in a relatively slow (∼0.1 c) magnetically controlled outflow. A curious dimming of the optical light is also apparent 2-5 s before the X-ray maximum. More detailed analyses of the optical response components, especially the mysterious "pre-cognition dip" were presented by [18] and [8].
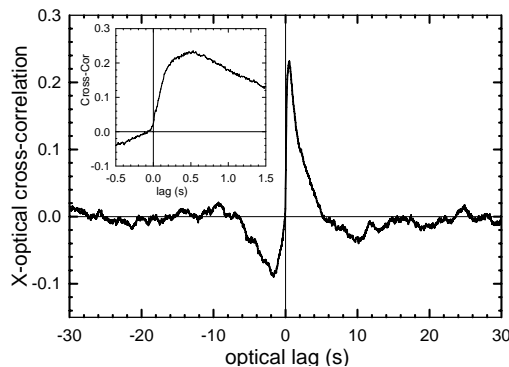
Fig. 14. The optical response correlated to X-ray variations of KV UMa (XTE J1118+48) shows time delayed emission and a preceding dip (pre-cognition dip)[4].

4 Conclusions

The scientific potential at the 'timing' frontier of astrophysics called 'high time resolution astronomy' (HTRA), can be well demonstrated by the observations performed with the small photo-polarimeter instrument OPTIMA. The fast ($\sim \mu s$) and sensitive (single photon detections) photometer is now augmented by options for polarimetry and coarse spectroscopy. In particular the observation of optical light from the vicinity of compact objects, like black holes, neutron stars, pulsars, and white dwarves has provided data on radiation processes in the most extreme astrophysical environments. The polarization measured in the Crab pulsar provides important constraints on the distribution and spectrum of high-energy electrons in the magnetosphere of a young pulsar. The absolute timing accuracy of OPTIMA allows correlated observations at different wavelengths with a precision of $\sim$ms. The multi-wavelength correlations obtained between the X-ray and optical band for the black hole binary system KV UMa in July 2000 showed very fast correlations between the variations in both ranges and revealed new and unexpected phenomena of radiation from the vicinity (jet, inner accretion disk) of a black hole.

The ongoing developments of fast ($\sim ms$) 2-dimensional detectors with high quantum efficiency over a wide spectral band (avalanche amplified pnC-CDs, e-m (electron multiplication) CCDs) and the 3-dimensional (location and energy) cryogenic detectors (tunnel junctions or transition edge sensors) will lead to the 'instruments of choice' for many scientific investigations in HTRA. The realm of ultrafast measurements will however still be covered best with single photon sensitive, discrete detectors. In the future we hope to adapt OPTIMA to the new, large telescopes and make use of their high light collecting power to investigate fainter sources with good statistics.

The discovery and investigation of optical counterparts to high-energy sources (bursts and steady sources in the gamma-ray range from sub MeV to TeV), which we expect from the current and near-future ground based (TeV imaging Cherenkov telescopes) and satellite observatories (SWIFT, INTEGRAL, AGILE, GLAST), will be an exciting field for all HTRA instruments. We also hope to contribute to these investigations with our suitably advanced OPTIMA.

References

1. Dyks, J., Rudak, B.: *ApJ*, **598**, 1201, (2003)
2. Dyks, J., Harding, A.K., Rudak, B.: *ApJ*, **606**, 1125, (2004)
3. Hester, J.J., P.A. Scowen, R. Sankrit, et al.: *ApJ*, **448**, 240, (1995)
4. Kanbach, G., Straubmeier, C., Spruit, H.C., Belloni, T., *Nature*, **414**, 180 (2001)
5. Kanbach, G., Slowikowska, A, Kellner, S., and Steinle, H.: AIP Conf. Proc. **801**, 306, *'Astrophysical Sources of High Energy Particles and Radiation'*, eds. T. Bulik, B. Rudak, and G. Madejski (2005)

6. Kellner, S. *Einsatz und Weiterentwicklung von OPTIMA als hochzeitauflösendes Photo- und Polarimeter (= Use and development of OPTIMA as a high time resolution Phot-Polarimeter), Diploma Thesis (in German) at the Technical University Munich*, (2002) available at http://www.mpe.mpg.de/gamma/instruments/optima/www/optima-papers.html

7. Lyne, A. G., Pritchard, R. S. & Roberts, M. E.: University of Manchester, Nuffield Radio Astronomy Laboratories, Jodrell Bank, Macclesfield, Cheshire, UK,(http://www.jb.ac.uk/ pulsar/crab.html) (1992)

8. Malzac J., Belloni T., Spruit H.C., Kanbach G.: *Astron. & Astrophys.*, **407**, 335 (2003)

9. D.D.E. Martin, P. Verhoeve , A. Peacock , et al: NIM-A **520**, 512 (2004)

10. Mühlegger, M. *Entwicklung und Einsatz eines Wollaston-Polarimeters für die Hochgeschindigkeitsastronomie mit OPTIMA-Burst (= Development and use of a Wollaston-polarimeter for high-time resolution astronomy with OPTIMA-Burst), Diploma Thesis (in German) at the Technical University Munich* (2006) available at http://www.mpe.mpg.de/gamma/instruments/optima/www/optima-papers.html

11. Ng, C.-Y. and R. Romani: *ApJ*, **644**, 445, (2006)

12. Percival, J. W., Biggs, J. D., Dolan, et al.: *ApJ*, **407**, 276 (1993)

13. Petri, J., Kirk, J.G.: *ApJ*, **627**, L37, (2005)

14. R.M. Redfern: Vistas Astron. **34**, 201 (1991)

15. Slowikowska, A., 'Pulsar Characteristics across the Energy Spectrum', PhD Thesis at the Nicolaus Copernicus Astronomical Center, Dept. of Astrophysics, Torun 2006, available at http://www.mpe.mpg.de/gamma/instruments/optima/www/optima-papers.html

16. Slowikowska, A., Kanbach, G., Stefanescu, A., *poster JD02-67 at XXVIth IAU GENERAL ASSEMBLY*, (2006)

17. Smith, F.G., Jones, D.H.P., Dick, J.S.B., Pike, C.D.: *MNRAS*, **233**, 305 (1988)

18. Spruit H.C. and Kanbach G.: *Astron.& Astrophys.*, **391**, 225 (2002)

19. Stefanescu, A. *Anpassung und Einsatz des OPTIMA Photometers zur Messung von GRB-Afterglow-Transienten (= Adaption and use of OPTIMA for the measurement of GRB-afterglow-transients), Diploma Thesis (in German) at the Technical University Munich* (2004) available at http://www.mpe.mpg.de/gamma/instruments/optima/www/optima-papers.html

20. Straubmeier, C., *OPTIMA - Entwicklung und erste astronomische Messungen eines optischen Hochgeschwindigkeitsphotometers (= OPTIMA - Development and first astronomical measurements with an optical high-speed photometer), Doctoral Thesis (in German) at the Technical University Munich* 2001, available at http://www.mpe.mpg.de/gamma/instruments/optima/www/optima-papers.html

21. C. Straubmeier, G. Kanbach, F. Schrey, *Exp. Astron.* **11**, 157 (2001)